MODELING HUMAN EXPOSURE TO PARTICLES IN INDOOR ENVIRONMENTS USING A DRIFT-FLUX MODEL

Gao Naiping[1], Niu Jianlei[1]

[1]Department of Building Science Engineering, The Hong Kong Polytechnic University, Hom Hung, Kowloon, Hong Kong, China,
Corresponding author: bejlniu@polyu.edu.hk (J.L. Niu)

ABSTRACT

This study developed a drift-flux model for particle movements in turbulent indoor airflows. To account for the process of particle deposition at solid boundaries in the numerical model, a semi-empirical deposition model was adopted in which the size-dependent deposition characteristics were well resolved. After validation against the experimental data, the drift-flux model was used to investigate human exposures to particles in three normally-used ventilation types: mixing ventilation (MV), displacement ventilation (DV), and under-floor air distribution (UFAD). The movements of submicron particles were like tracer gases while the gravitational settling effect should be taken into account for particles larger than 2.5 um. For particles released from an internal heat source, the concentration stratification of small particles (diameter <10 um) in the vertical direction appeared in DV and UFAD. It was found the advantageous principle for gaseous pollutants that a relatively less-polluted occupied zone existed in DV and UFAD was also applicable to small particles.

KEYWORDS

Drift-flux model, Particle, Exposure, Mixing ventilation, Displacement ventilation, Under-floor air distribution

INTRODUCTION

The emergence of severe acute respiratory syndrome (SARS), the unremitting threat of avian influenza, and the possible terrorist attacks by airborne release of aerosolized chemical or biological agents into a building generate more concerns on the study of particles/droplets movement indoors. Several reports have shown that many infectious diseases can be transmitted via the airborne route (Nardell et al. 1986; Mangili and Gendreau 2005). A recent multidisciplinary systematic review reveals that there is a strong and sufficient evidence to demonstrate the association between ventilation, airflow pattern in buildings and the spread of infectious diseases (Li et al. 2007). Besides human-generated virus laden bio-aerosols, smoke particles could increase respiratory irritation and aggravation of existing respiratory or cardiovascular disease, an asbestos fiber exposure for prolonged periods increases the risk of lung cancer, and miner aerosols may be carcinogenic or mutagenic. Generally the health hazards caused by particulate matter depend on the component, size, shape, density, and chemical reactivity of the particles.

Mathematically, there are two treatments of indoor particle movements: the Euler-Lagrange method and the Euler-Euler method. The selection between them is based on the "job" (research objective) and the "cost" (required computational resources) (Loth 2000). Generally the Lagrangian method may be comparatively memory intensive and computationally inefficient in order to ensure statistically stable results. However, the Lagrangian method is attractive if interests are in the particle dispersion history. In addition, particle reflection from the surface, coagulation and evaporation process, and poly-dispersion of size can be incorporated. Holmberg and Li (1998) have justified the two application requirements of the Euler-Euler method in the modeling of indoor environments. These are the particle size should be significantly smaller than the Kolmogorow microscale and there should be enough particles in each computational cell so that the particle phase can be statistically assumed as a continuum. The Kolmogorow microscale is at the magnitude of 1 mm for a normal ventilated room (Etheridge and Sandberg 1996), which is at least several times of indoor particle sizes. The interaction between particles and airstreams in built environments is considered as one-way coupling for saving computational load. It means a dilute dispersed phase flow, in which particle movements are determined by the state of the airflow. Both the transfer of momentum and heat from particles to fluids and particle-particle interactions are ignored. For this treatment to be valid, the particulate loading should be low since it has a significant impact on phase interaction.

In this paper, one kind of simplified Eulerian method, i.e. a drift-flux model, is used to investigate particle distribution in an enclosed environment. The purpose of this work is to improve the wall boundary treatment in the drift-flux model with the help of one deposition model. After validation against

experimental data, the new drift-flux model is applied to compare the occupant exposures to particles generated from a heat source in a ventilated room with mixing ventilation (MV), displacement ventilation (DV), and under-floor air distribution (UFAD).

METHODS

Drift-flux model

The drift-flux model is not a fully-coupled multi-fluid model. The governing equation of the particle concentration is similar to Navier-Stokes equations, except that it integrates the gravitational settling effect of particles into the convection term.

$$\frac{\partial(\rho C)}{\partial t}+\nabla\bullet(\rho(\vec{V}+\overrightarrow{V_S})C)=\nabla\bullet(\frac{\mu_{eff}}{\sigma_C}\nabla C)+S_C \quad (1)$$

The gravitational settling velocity of particles ($\overrightarrow{V_S}$) is calculated by Stokes equation. Here σ_C is set as 1.0. The term $\frac{\mu_{eff}}{\sigma_C}$ can also be written as $D_p+\varepsilon_P$. Equation 1 is discretized directly into algebraic equation by the finite volume method, not like the other numerical treatment in which the settling term $\rho\overline{V}_s C$ is removed into the source term. In the progress of CFD calculation, the indoor flow field and temperature field are solved firstly using standard k- ε model including buoyancy effect plus standard wall function. After convergence is reached, Equation 1 is solved solely due to the one-way coupling.

Particle deposition

To quantify the deposition in the engineering calculation, some prediction models have been set up. The semi-empirical model by Lai and Nazaroff (2000) links the air velocity to the macro-deposition velocity, with no consideration given the effect of spatial distribution of particles. This model accounts for the effects of Brownian and turbulent diffusion and gravitational settling. With the assumption that the deposition flux is one-dimensional and constant in the concentration boundary layer, and the particle eddy diffusivity equals the fluid turbulent viscosity ($\varepsilon_p=\upsilon_t$), the dimensionless deposition velocity can be expressed by the following equation:

$$v_d^+=\begin{cases}\dfrac{v_s^+}{1-\exp(-v_s^+ I)}, & \text{upward surface}\\ \dfrac{v_s^+}{\exp(-v_s^+ I)-1}, & \text{downdard surface}\\ \dfrac{u^*}{I}, & \text{vertical surface}\end{cases} \quad (2)$$

Where $v_s^+=\frac{v_s}{u^*}$, $v_d^+=\frac{v_d}{u^*}$,

$$I=\frac{1}{v_d^+}=\int_{r^+}^{30}\left(\frac{\upsilon_g}{\varepsilon_p+D_p}\right)dy^+ \quad , \quad y^+=\frac{yu^*}{\upsilon_g} \quad ,$$

$$r^+=\left(\frac{D}{2}\right)\left(\frac{u^*}{\upsilon_g}\right)$$

In their derivation, the turbulent viscosity in the boundary layer is evaluated by the DNS results of Kim et al. (1987). This model is practical to use yet have a stronger physical foundation if comparing with previous ones.

Boundary condition

Different from dealing with the governing equation of a tracer gas where a zero-flux condition can be assumed at the solid boundary, particle deposition should be taken into account at the walls since a net transport of particles towards walls creates concentration gradients (Figure 1). Zhao et al. (2004) assumed $\partial C/\partial n=0$ at walls for particles. In the work by Holmberg and Li (1998), they considered C_{wall} as αC_{cell} $(0\le\alpha\le 1)$. The appropriate value of α was obtained from deposition measurement. In present work, the Lai and Nazaroff's model is used to evaluate deposition velocities (Lai and Nazaroff 2000). Since the deposition flux is define as $J=v_d C_{cell}=(D_p+\varepsilon_P)\frac{dC}{dy}+iv_s C_{cell}$, the particle concentration at walls can be expressed as

$$C_{wall}=C_{cell}-C_{cell}(v_d-iv_s)\frac{dy}{(D_p+\varepsilon_P)} \quad (3)$$

by using $\frac{C_{cell}-C_{wall}}{dy}$ to substitute $\frac{dC}{dy}$, where i is to characterize the wall surface orientation ($i=0$ for a vertical surface; $i=1$ for an upward facing horizontal surface; $i=-1$ for a downward facing horizontal surface). In our simulation using Equation 3, it is found that usually the particle concentration gradient is highest at downward facing surfaces, and lowest at upward facing surfaces. It is in line with the modeling of aerosol in a chamber by Holmberg and

Li (1998). They found the α values were 0.9, 0.99, and 0.65 for walls, floor, and ceiling respectively. This approximate zero-gradient of particle concentration at floor means that particle deposition at floor is mainly caused by gravitational settling, not by diffusion. For particles larger than 0.5 um, the deposition velocity is nearly the same as the settling velocity and the effect of local airflow condition (denoted by the friction velocity) can be ignored (Figure 4 in Lai and Nazaroff 2000). However it should be mentioned that present treatment of solid boundary still need to be improved. First, C_{wall} value is grid-dependent. The first normal grid point should be located beyond the buffer layer ($y^+ > 30$). Second, this deposition model usually under-predicts the deposition flux onto the downward facing surfaces, especially for coarse particles. Maybe other deposition mechanisms, other than diffusion, gravitational settling, and turbophoresis, also play an important role. Here it demands the further development of enhanced deposition models.

VALIDATION

Chen et al. (2006) measured the concentration of mono-dispersed 10 um particle with a material density of 1400 kg/m^3 in a simple model room (Figure 2). Particles were mixed into the supply air with a stable particle flow rate by a solid particle disperser. Particle concentration is normalized by the inlet concentration, which is considered to be uniform. Since the air is supplied at the ceiling level and exhausted at the floor level, one large eddy and a small recirculation zone at the left lower corner are formed. The simulated and measured concentration profiles are compared in Figure 3. Because the airflow field in this experiment was comparatively simple and it was isothermal, a fine agreement is achieved.

Zhang and Chen (2006) carried out an experimental study on indoor particle dispersion in a full-scale environmental chamber with UFAD (Figure 4). Air was supplied to the chamber at a total flow rate of 0.0944 m^3/s by two openings located on the floor, and was exhausted at the ceiling. Four heated manikins and six lamps installed on the ceiling were used to simulate heat sources in a normal room. Liquid droplets with a low evaporation rate were introduced by a carrier gas (nitrogen, at a flow rate of $7*10^{-5}$ m^3/s) into the room at a position 0.3 m above the floor (X=1.5m, Y=2.1m, Z=0.3m). The diameter of the mono-disperse spherical particles was 0.7 um. Particle concentrations were monitored at the exhaust outlet, and at five height levels (0.4m, 0.8m, 1.2m, 1.6m, 1.8m) of six locations (from P1 to P6 as shown in Figure 4).

Temporal evolution of particle concentration at the exhaust is modeled (Figure 5). At time t=0 min, particle emission is initiated at a steady flux. The stable concentration at the exhaust is denoted as 1.0. The numerical prediction is in accord with the experimental data. The time required to reach the stable outlet concentration is obviously dependent on the particle release location. If the particle is generated in a recirculation zone, or so called a dead zone, it can be imaged that it takes a longer time to be ventilated out of the room. Here the concept of residual life time can be employed. In a pulse emission of n particles, if the portion of the particles that can arrive at the exhaust is α and each particle takes time t_i, the particle residual life time can be defined as

$$\tau_r = \frac{\sum_{1}^{\alpha \times n} t_i}{\alpha \times n} \quad (4)$$

We replaced the 0.7um particles by a tracer gas or other coarse particles (7um, 14um, and 21um) and simulated temporal development of exhaust concentration for comparison. The time required to arrive at stable concentration is almost the same. Previous studies in a channel flow ((Brandon and Aggarwal 2001)) and in free shear layers (Loth 1998) have revealed that particle dispersion depends on Stokes number (S_t) which is the ratio of particle response time to characteristic time. Particles with $S_t < 0.1$ behave like fluid particles, whereas those with $S_t \approx 1.0$ no longer faithfully follow the trajectories of fluid particles but can still respond readily to fluid velocity fluctuations and those with $S_t > 1.0$ diffuse at a much slower rate than that of a scalar field inasmuch as their inertia is too great to be significantly affected by the turbulent dispersion. The experiment by Hishida et al. (1992) confirmed that with $S_t \sim O(1)$ particle dispersion coefficients became larger than the eddy diffusivity of the fluid phase. However since the particle turbulent diffusivity is expressed by fluid turbulent viscosity this phenomenon is not evidently captured by present drift-flux model.

APPLICATION

Case description

In this section, using the aforementioned drift-flux model, we aim to compare human exposures in various air distribution systems, such as mixing ventilation (MV), displacement ventilation (DV), and under-floor air distribution (UFAD). A room configuration has been demonstrated in our former study of the effect of personalized ventilation on thermal comfort and inhaled air quality (Gao et al. 2007). In the simulations we used a breathing numerical thermal manikin (NTM) with nose and

mouth. All the body features were represented by this NTM. The NTM was seated in a room with the dimensions of 4.0m (length) X 3.0m (width) X 2.7m (height) (Figure 6). Two types of ventilation systems were installed, i.e. mixing and displacement ventilation systems. With displacement ventilation, a large wall-mounted diffuser was located at the floor level to supply cool air at a low speed, and an exhaust at the ceiling level. For mixing ventilation, an inlet diffuser with small opening was set at the upper level, and an outlet at the floor level. A vertical heat source beside the desk was specially designed to create different level of vertical thermal stratification. The workplace was equipped with a personalized ventilation system which was simply represented by one circular air terminal device with a diameter of 20 cm. In this study, the personalized ventilation is removed while an UFAD is added.

The Navier-Stokes equations are solved based on a finite-volume method. The numerical methods and boundary conditions are summarized in Table 1. The simulated results of velocity and temperature distributions have been discussed before (Gao et al. 2007). Here highlighted are the concentration distributions of particles whose material density is 1000 kg/m^3. The particles are uniformly released from the vertical heat source (item 2 in Figure 6) at a rate of 0.154 ug/s.

Human exposure

The particle concentrations and air temperatures at different height levels at one location behind the human body (X=2.8m, Y=1.5m) are illustrated in Figure 7. In MV particle concentration is almost uniform except at the points close to the ceiling where there is a clean supply airflow. The higher particle diameters, the lower mean indoor concentrations. For particles smaller than 5.0um, human exposure is nearly equal to the outlet concentration. However for larger particles, human exposure is much less than the outlet concentration due to the aspiration efficiency. In DV a vertical concentration stratification is observed. It is shown that the buoyant upward airflows in a displacement ventilated room are able to bring the particles to the upper zone. Because of the heavy gravitation, this principle can not be applied to 20um particles. Human exposure is greatly lower than that in MV for 0.1, 1.0, 2.5, and 5.0um particles, but larger for 10.0 and 20.0um particle. Like treating with non-passive gaseous pollutants, DV is still preferable to MV as to fine particles. We suspect that a portion of 10.0 and 20.0um particles, which are too heavy to be carried up, are locked in the breathing height, resulting in a higher exposure in DV. In UFAD the vertical stratification for 0.1, 1.0, and 2.5um particle also appears and human exposure is slightly higher than in DV. But owing to the weak carry-up effect, particles larger than 5.0um are unable to be entrained to the upper level.

The distinct particle distributions in these three ventilation methods are a consequence of different indoor airflow patterns. It is easy to understand that in MV a strong jet flow with a high momentum causes a fully mixing of indoor air. In comparison to DV where supply air is delivered at low velocities, UFAD systems deliver air through floor diffusers at higher velocities. In order to reduce the local drafts at low levels, floor air outlets are designed to maximize air mixing within the occupied zone, which diminishes the ventilation performance compared to DV systems. This is why the concentration closely above the floor in DV (see Figure 7b) is almost zero while on the contrary it is not true in UFAD. With UFAD systems, the thermal plumes generated from heat sources are a minor, secondary characteristic of the system, with the primary air motion in the occupied zone created by the high velocity floor diffuser (McDonell 2003). However, DV systems are designed to minimize the mixing of air in the occupied zone, and thermal plumes are the dominant air movement characteristic. Room air is displaced out at a higher portion of the space by continual supply of fresh air. As shown by Figure 7(d), a steeper vertical temperature gradient is formed in DV than in UFAD, and the temperatures of air close to the floor is higher in UFAD, since swirling diffuser is characterized by a swirling discharge airflow pattern that is intended to produce high induction and limited throws (Webster et al. 2002). This steeper temperature gradient induces a stronger carry-up effect in DV.

CONCLUSION

In this study a simplified Eulerian method, i.e. a drift-flux model, is developed with an improvement on the solid boundary condition with the help of a semi-empirical deposition model. After validated against the experimental measurements in a scaled isothermal chamber and in a full-scale non-isothermal environmental chamber, the drift-flux model is used to compare human exposures to particles from indoor sources in mixing ventilation, displacement ventilation, and under-floor air distribution. Vertical concentration stratification appears in DV and UFAD for particles up to 10.0um. The advantageous principle of DV and UFAD that there is a less polluted occupied zone for non-passive gaseous pollutants is also applicable to particles whose diameters are less than a certain value which depending on the strength of the buoyancy force.

Although some meaningful results have been obtained, present numerical method still needs to be improved further. For example, application of concentrations in the first normal cells makes the deposition flux is grid-dependent. And the diffusion

term in the governing equation of concentration can not resolve the size-dependent dispersion characteristics.

NOMENCLATURE

C	particle mass concentration
C_{cell}	particle concentration in the first cell normal to the wall
C_{wall}	particle concentration at the walls
D	particle diameter
D_p	Brownian diffusivity
S_c	particle source term
S_t	Stokes number
t	time
$u*$	friction velocity
$\vec{V}$	vector of air velocity
$\overrightarrow{V_s}$	vector of particle settling velocity
v_d	particle deposition velocity
v_s	particle settling velocity
y	the normal distance between the wall and the first cell center
ε_p	turbulent diffusivity
υ_g	kinetic air viscosity
μ_{eff}	effective viscosity
ρ	the density of the air
σ_c	non-dimensional number

REFERENCES

Brandon DJ, and Aggarwal SK. 2001. "A numerical investigation of particle deposition on a square cylinder placed in a channel flow," Aerosol Science and Technology. 34: 340-352.

Chen F, Yu SCM, and Lai ACK. 2006. "Modeling particle distribution and deposition in indoor environments with a new drift-flux model," Atmospheric Environment. 40: 357-367.

Etheridge D, Sandberg M. 1996. Building Ventilation: Theory and Measurement. Chichester, John Wiley & Sons.

Gao NP, Zhang H, and Niu JL. 2007. "Investigating indoor air quality and thermal comfort using a numerical thermal manikin," Indoor and Built Environment. 16(1): 7-17.

Hishida H, Ando A, and Maeda M. 1992. "Experiments on particle dispersion in a turbulent mixing layer," International Journal of Multiphase Flow. 18: 181-194.

Holmberg S, and Li Y. 1998. "Modelling of the indoor environment-particle dispersion and deposition," Indoor Air. 8: 113-122.

Kim J, Moin P, and Moser R. 1987. "Turbulence statistics in fully developed channel flow at low Reynolds number," Journal of Fluid Mechanics. 177: 133-166.

Lai ACK, and Nazaroff WW. 2000. "Modeling indoor particle deposition from turbulent flow onto smooth surfaces," Journal of Aerosol Science. 31: 463-476.

Li Y, Leung GM, Tang JW, Yang X, Chao C, Lin JZ, Lu JW, Nielsen PV, Niu J, Qian H, Sleigh AC, Su HJ, Sundell J, Wong TW, and Yeun PL. 2007. "Role of ventilation in airborne transmission of infectious agents in the built environment- a multidisciplinary systematic review," Indoor Air. 17(1): 2-18.

Loth E. 1998. "Eulerian model for mean turbulent diffusion of particles in free shear layers," AIAA Journal. 36: 12-17.

Loth E. 2000. "Numerical approaches for motion of dispersed particles, droplets and bubbles," Progress in Energy and Combustion Science. 26: 161-223

Mangili A, and Gendreau MA. 2005. "Transmission of infectious diseases during commercial air travel," Lancet. 365: 989-994.

McDonell G. 2003. "Underfloor & displacement: why they're not the same," ASHRAE Journal. 45: 18-24.

Nardell EA, McInnis B, Thomas B, Weidhaas S. 1986. "Exogenous reinfection with tuberculosis in a shelter for the homeless," New England Journal of Medicine. 315: 1570-1575.

Webster T, Bauman F, Reese J. 2002. "Underfloor air distribution: thermal stratification," ASHRAE Journal. 44: 28-30+32+34+36.

Zhang Z, and Chen Q. 2006. "Experimental measurements and numerical simulations of particle transport and distribution in ventilated rooms," Atmospheric Environment. 40: 3396-3408.

Zhao B, Li X, Zhang Z, and Huang D. 2004. "Comparison of diffusion characteristics of aerosol particles in different ventilated rooms by numerical method," ASHRAE Transactions. 110: 88-95.

FIGURES AND TABLES

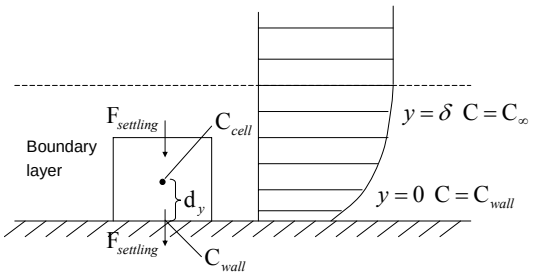

Figure 1 Boundary conditions of the near wall particle concentration field

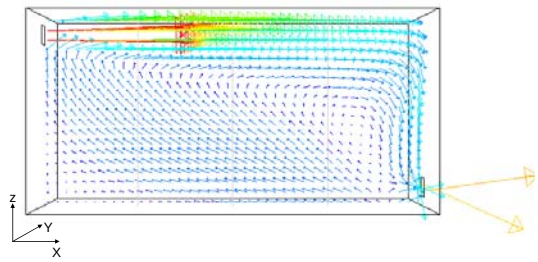

Figure 2 Airflow pattern at the centre plane (Y=0.2m) of the model room (X0.8m, Y0.4m, Z0.4m), the inlet and outlet are 0.04m×0.04m, the inlet air velocity is 0.225 m/s.

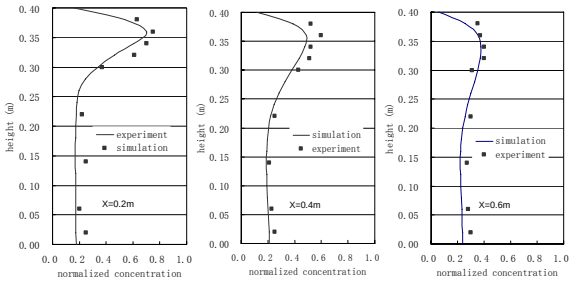

Figure 3 A comparison of simulated and measured particle concentrations at the centre plane

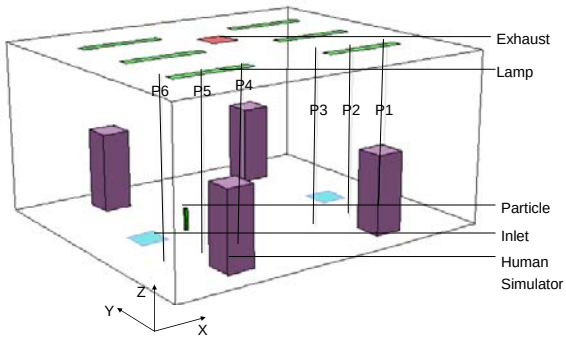

Figure 4 A sketch of the environmental chamber configuration (X4.8m, Y4.2m, Z2.4m)

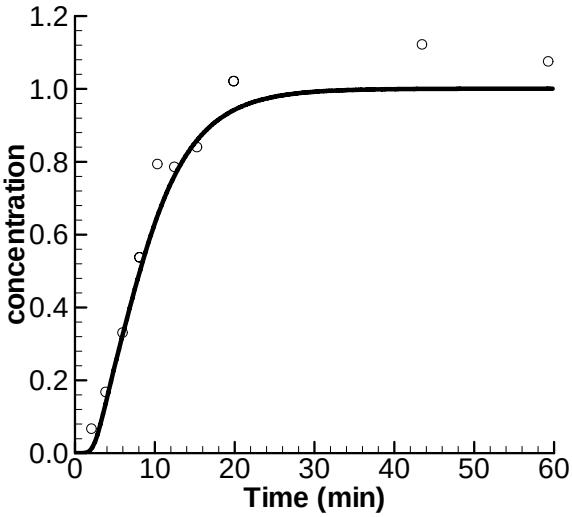

Figure 5 Simulated and measured temporal normalized concentration at the exhaust (cycle: experimental data; curve line: simulations)

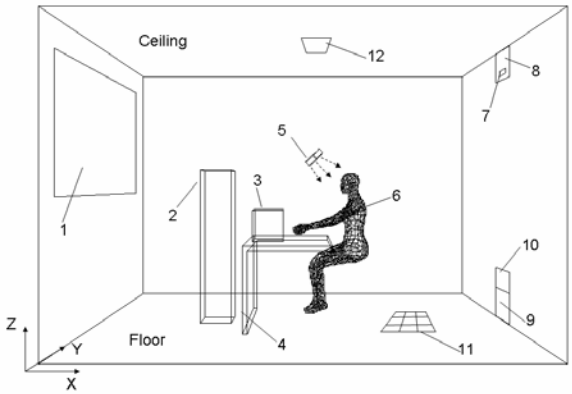

Figure 6 Configuration of the simulated office (room length (X) 4m, width (Y) 3m, height (Z) 2.7m; 1-window; 2-vertical heat source; 3-computer; 4-table; 5-personalized ventilation air terminal device (circular outlet with a diameter of 20 cm); 6-human body; 7-mixing ventilation inlet 0.2m×0.05m; 8-displacement ventilation outlet 0.4m×0.3m; 9-mixing ventilation outlet 0.4m×0.3m; 10-displacement ventilation inlet 0.4m×0.5m; 11-UFAD inlet 0.21m×0.21m; 12-UFAD outlet 0.4m×0.4m)

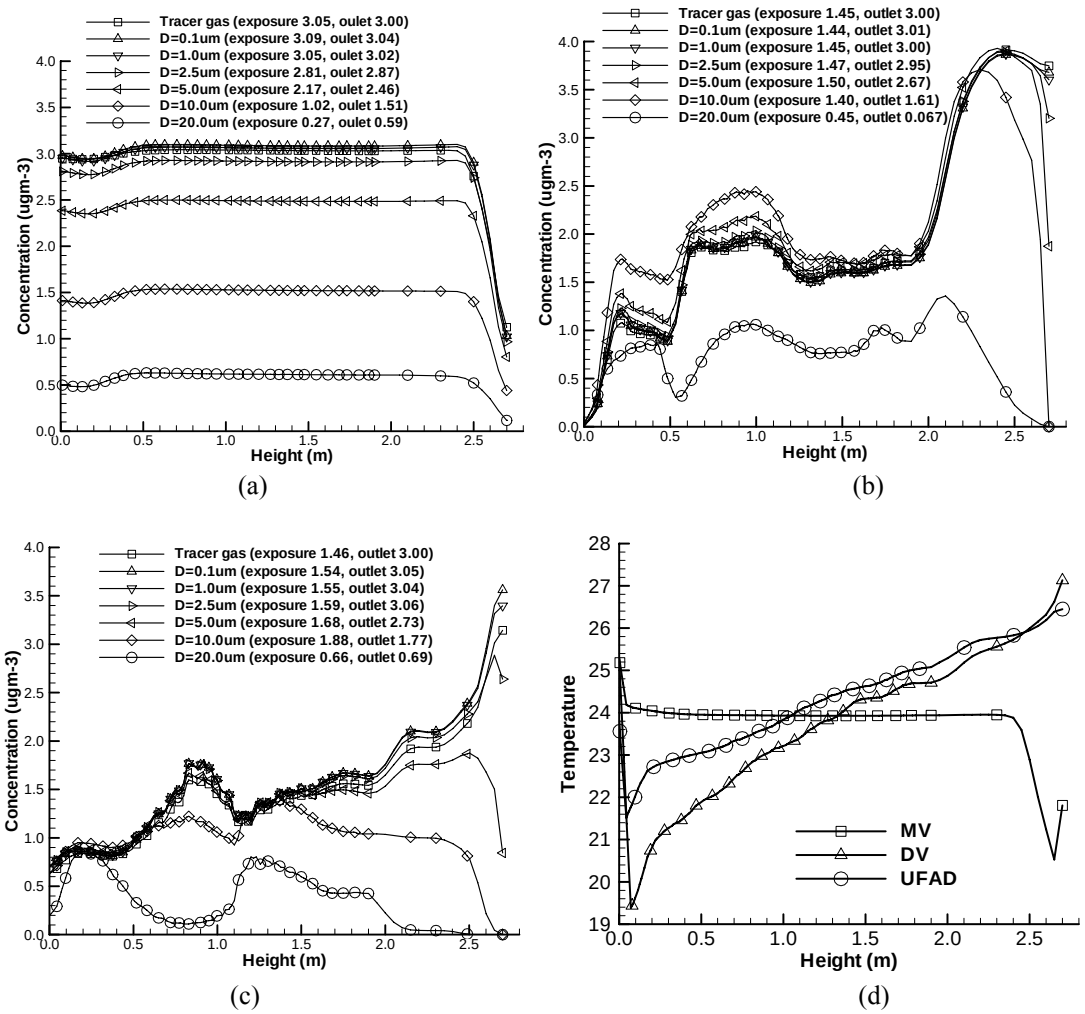

Figure 7 Vertical distribution of particle concentration where the particles are generated from the heat source in the MV room (a), DV room (b), and UFAD room (c), and vertical temperature distribution (d)

Table 1. The details of numerical methods

Turbulence Model	Standard k-ε model
Numerical Schemes	Upwind second order difference for the convection term; SIMPLEC algorithm
Window	Uniform heat flux 150W
Floor, ceiling, walls	Adiabatic wall
Vertical heat source	Uniform heat flux 100W
Human body	Fixed skin temperatures at 31℃
Computer	Uniform heat flux 120W
Table	Adiabatic wall
MV inlet	Airflow rate 51l/s, turbulence intensity 30%, turbulence length scale 0.005m, 19℃
DV inlet	Airflow rate 51l/s, turbulence intensity 15%, turbulence length scale 0.03m, 19℃
UFAD inlet	Airflow rate 51l/s, turbulence intensity 15%, turbulence length scale 0.03m, 19℃
MV/DV/UFAD outlet	Velocity and temperature: free slip
Nose	Steady inhalation, respiration rate 8.4 l/min, turbulence intensity 20%, hydraulic diameter 0.01m